Designing Higher Surface Area Metal−Organic Frameworks: Are Triple Bonds Better Than Phenyls?

Omar K. Farha,[*,†,∥] Christopher E. Wilmer,[‡,∥] Ibrahim Eryazici,[†,∥] Brad G. Hauser,[†] Philip A. Parilla,[§] Kevin O'Neill,[§] Amy A. Sarjeant,[†] SonBinh T. Nguyen,[†] Randall Q. Snurr,[*,‡] and Joseph T. Hupp[*,†]

[†]Department of Chemistry and International Institute for Nanotechnology, Northwestern University, 2145 Sheridan Road, Evanston, Illinois 60208-3113, United States

[‡]Department of Chemical & Biological Engineering, Northwestern University, 2145 Sheridan Road, Evanston, Illinois 60208-3120, United States

[§]National Renewable Energy Laboratory, Golden, Colorado 80401, United States

Ⓢ *Supporting Information*

ABSTRACT: We have synthesized, characterized, and computationally validated the high Brunauer−Emmett−Teller surface area and hydrogen uptake of a new, noncatenating metal−organic framework (MOF) material, **NU-111**. Our results imply that replacing the phenyl spacers of organic linkers with triple-bond spacers is an effective strategy for boosting molecule-accessible gravimetric surface areas of MOFs and related high-porosity materials.

The chemical and structural diversity of metal−organic frameworks (MOFs) is one of the most notable characteristics of these materials. MOFs are hybrid materials composed of inorganic nodes and organic struts.[1−3] The most intriguing examples exhibit large internal surface areas; ultralow densities; uniform channels, cavities, and voids; and permanent porosity. Because of these exceptional properties, MOFs are being investigated for many potential applications, including gas storage,[4−8] gas and chemical separations,[9−12] chemical catalysis,[13,14] sensing,[15] ion exchange,[16] drug delivery,[17] and light harvesting.[18,19] Furthermore, the availability of single-crystal structures of MOFs allows the use of computational modeling to calculate guest adsorption capabilities and other properties, which can help in screening MOFs for particular applications and improving our understanding of their performance.[20] The fact that these computational methods can be usefully applied gives MOFs a significant advantage over their amorphous counterparts.

Rising concerns about climate change have intensified the search for environmentally friendly and renewable fuels such as water-derived H_2, cellulosic ethanol, and photo- or electro-chemically generated methane. Although molecular hydrogen is a compelling alternative to gasoline in many respects, high-density storage is a significant challenge for the viability of hydrogen-powered vehicles. In order to drive 300 miles, 5 to 13 kg of H_2 are needed. Therefore, technologies that can efficiently concentrate gases at lower pressures, such as adsorption on porous materials, are desirable. The U.S. Department of Energy (DOE) has set targets for on-board H_2 storage systems for the year 2017: 5.5 wt % in gravimetric capacity and 40 g/L of

volumetric capacity at an operating temperature in the range −40 to 60 °C under a maximum delivery pressure of 100 atm.[21] Recently, automobile manufacturer Mercedes-Benz has announced its intention to use MOFs for mobile hydrogen storage at *cryogenic* temperatures.[22] Required are materials with surface areas of ∼24 million square feet of surface area per pound (4900 m^2/g) and the ability to store substantial hydrogen at 435 psi (30 bar). MOFs are powerful contenders relative to other porous materials in meeting these conditions.

We set out to make a MOF that satisfies both of the aforementioned requirements (∼4900 m^2/g and high hydrogen uptake at 30 bar). We turned our attention to (3,24)-paddlewheel-connected MOF networks (*rht* topology),[23] for which catenation (interpenetration or interweaving of multiple frameworks) is impossible. The use of this topology was pioneered by Eddaoudi[23] and has been used by us[24] and the Zhou[25] and Schröder[26] groups. Recently, a MOF denoted as either **PCN-69**[27] or **NOTT-119**[28] with the *rht* topology was synthesized by both the Zhou and Schroder groups. **PCN-69/NOTT-119** has a Brunauer−Emmett−Teller (BET) surface area of ∼4000 m^2/g and is made from the phenyl-based strut **LH₆(1)** (Scheme 1). Even though **LH₆(1)** is longer than

Scheme 1. Hexacarboxylic Acid Struts Used To Construct PCN-69/NOTT-119 [LH₆(1)], NOTT-112 [LH₆(2)], and NU-111 [LH₆(3)]
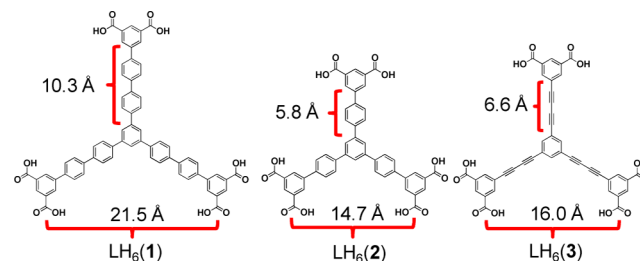
LH₆(2), the strut used to make **NOTT-112**[26] (3800 m^2/g), the surface area of **PCN-69/NOTT-119** did not increase significantly. To date, the best known strategy for obtaining

higher-surface-area MOFs has been to use longer linkers.[24,29] However, as the case of **PCN-69/NOTT-119** shows, it is not only the length of the linker but also the shape and density that matter for high surface area.

With the above considerations in mind, we decided to replace the two phenyl spacers in each arm of the linker in **PCN-69/NOTT-119** with two triple-bond spacers. Our initial notions were based on hypothetically exposing the edges of phenyl spacers by dividing each linker arm into three individual but chemically linked pieces, each consisting of two carbon atoms linked by a triple bond. These pieces are equivalent to acetylenes, but with carbon−carbon single bonds to neighboring pieces replacing the terminal hydrogen atoms. Thus, six linked alkynes would replace two linked phenyl groups. Given the synthetic challenge presented by the corresponding trigonal linker, however, we chose instead to start by replacing each phenyl spacer in **LH$_6$(1)** by one carbon−carbon triple bond.

In this report, we describe the synthesis and properties of a new MOF, **NU-111** (**NU** = Northwestern University), formed from the new hexacarboxylic acid linker **LH$_6$(3)** that contains three pairs of triple-bond spacers. The synthesis and characterization of **LH$_6$(3)** is described in the Supporting Information (SI). Briefly, **LH$_6$(3)** was obtained via saponification of the corresponding hexaester precursor, which in turn was obtained via Sonogashira coupling of 1,3,5-triiodobenzene with 1,3-diethoxycarbonyl-5-(butadiynyl)benzene.

Solvothermal reactions of **LH$_6$(3)** and Cu(NO$_3$)$_2$·2.5H$_2$O in DMF/EtOH/HCl (DMF = dimethylformamide) at 80 °C gave MOFs with the framework formula $[Cu_3(L(3))(H_2O)_3]_n$ in 75% yield after 48 h. X-ray analysis of single crystals of **NU-111** revealed a noncatenated structure with a cubic space group, $Fm\overline{3}m$, in which the framework nodes consist of Cu$^{II}_2$ units coordinated by the carboxylates of **L(3)$^{6-}$** in paddlewheel fashion (Figure 1A,B). The axial sites of the Cu$^{II}_2$ units are coordinated by water molecules that were well-resolved in the X-ray analysis. The experimental structure has unit-cell dimensions of $a = b = c = 48.9$ Å at 225 K. **NU-111** can be represented using three types of space-filling polyhedra (also termed cages) that are derived from drawing straight lines between copper paddlewheels (Figure 2B−D column 1) and are fused in such a way that they form continuous channels (Figure 2E). The smallest cage is cuboctahedral and is formed from 24 isophthalate groups from **L(3)$^{6-}$** units and 12 pairs of copper ions (Figure 2B). The second cage is a truncated tetrahedron and is formed from isophthalate groups from four **L(3)$^{6-}$** linkers and 12 pairs of copper ions (Figure 2C). The largest cage can be described as a truncated cuboctahedron and is formed by 24 Cu$^{II}_2$ paddlewheel nodes and portions of eight distinct **L(3)$^{6-}$** units (Figure 2D). However, there is no unique representation of a MOF in the form of space-filling polyhedra, and the scheme described above, though both common and useful for *rht* topologies, neglects an important feature of **NU-111**: a fourth cavity that can be detected experimentally (Figure 1C, blue). An alternate choice of space-filling polyhedra can lead to greater physical insight; in this case, taking the curvature of the ligand into account gives four types of polyhedral cages, each corresponding to one of the four experimentally discovered cavities (Figure 2A−D column 2 and Figure 2F). Therefore, there are two ways of describing the topological features of **NU-111** (see Figures S21 and S22 in the SI). The phase purity of a bulk sample of **NU-111** was established via powder X-ray diffraction (PXRD) measurements since the simulated PXRD pattern was found to be in excellent
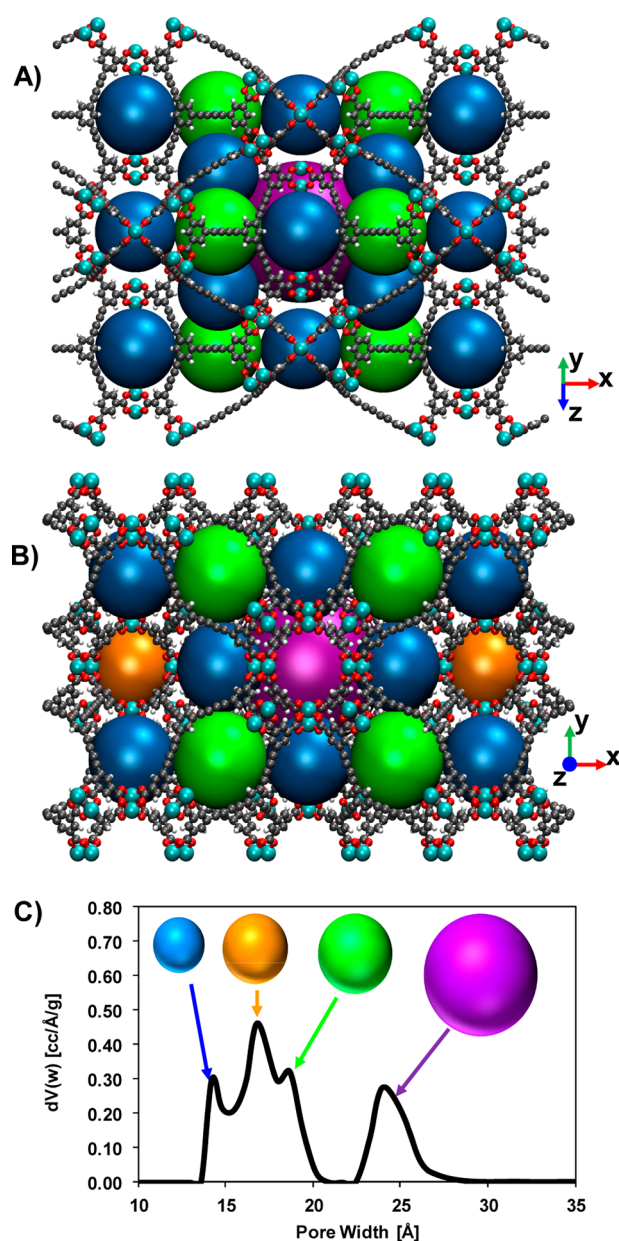

Figure 1. (A, B) Structurally derived views of **NU-111**. (C) Calculated pore size distribution of **NU-111** based on experimental Ar adsorption at 87 K. DFT kernel used: Ar at 87 K_zeolites/silica (cylindrical pore, NLDFT equilibrium model).

agreement with the experimental one (Figure S11). Additionally, thermogravimetric analysis (TGA) of **NU-111** revealed a mass loss at ~135 °C assigned to solvent (DMF), and no further mass loss occurred until ~300 °C (Figure S12).

After the guest solvent molecules were removed using supercritical CO$_2$[29-33] (see the SI for activation details), the porosity was examined by nitrogen adsorption at 77 K. The experimental and simulated N$_2$ isotherms were in excellent agreement, as shown in Figure 3A. The experimental BET surface area of **NU-111** was found to be 5000 ± 80 m^2/g, which is higher than that of **PCN-69/NOTT-119** (3989/4118 m^2/g). It is worth mentioning that the experimental BET surface area is in excellent agreement with that determined from the computationally simulated isotherm (4915 m^2/g). The total experimental pore volume of **NU-111** is 2.38 cm^3/g. The pore size distribution of **NU-111**, calculated from Ar
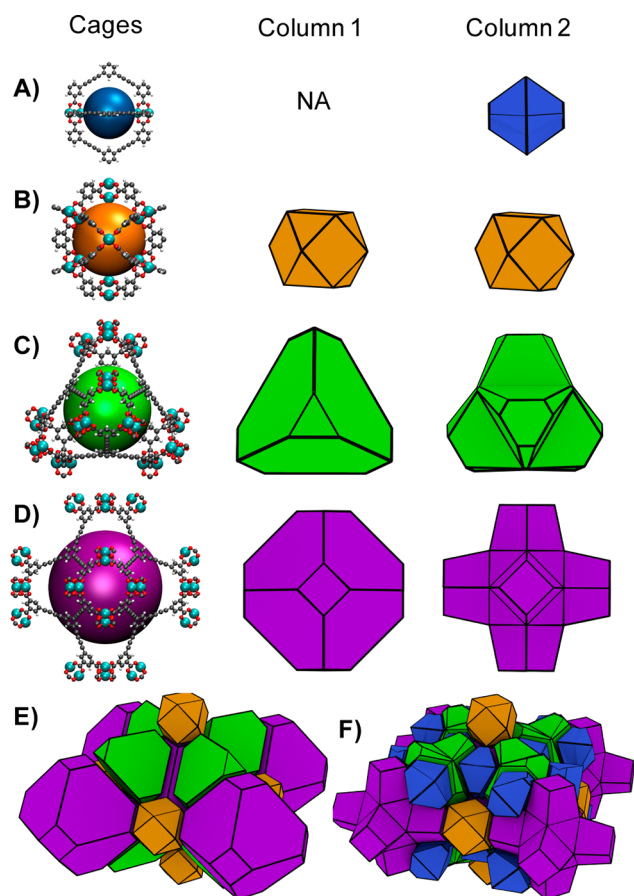
Figure 2. (A–D) Polyhedra in **NU-111** obtained by drawing straight lines between the copper paddlewheels (column 1) and by taking into account the curvature of the ligands (column 2). (E, F) Packing of the polyhedra shown in (E) column 1 and (F) column 2. Color code: Cu, teal; C, gray; O, red; H, white.

Figure 3. Adsorption isotherms of **NU-111** at 77 K: (A) N_2 isotherms; (B) excess H_2 isotherms; (C) excess and absolute (total) H_2 isotherms.

adsorption experiments at 87 K using nonlocal density functional theory (NLDFT), shows peaks at 14, 17, 19, and 24 Å (Figure 1C), in excellent agreement with a geometric calculation based on the crystal structure (Figure S19).

The large surface area and pore volume of **NU-111** prompted us to measure its high-pressure hydrogen capacity. These measurements were done at the DOE Hydrogen Sorption Center of Excellence at the National Renewable Energy Laboratory (NREL). Sorption data for H_2 were collected up to 110 bar at 77 K. It should be noted that only the "excess" gas adsorption is directly accessible experimentally. Excess gas adsorption is the amount adsorbed as a result of the presence of the adsorbent. The total adsorption is the sum of the excess adsorption and the amount that would be found within the pore volume, on the basis of the finite bulk-phase density of the gas, if the adsorbent were not present. For gas storage and delivery purposes, the total amount adsorbed is the more relevant quantity. The excess hydrogen uptake of **NU-111** was 21 mg/g at 1 bar and 69 mg/g at 32 bar (Figure 3B and Figure S23). From the N_2-derived pore volume (2.38 cm^3/ g) and the bulk phase density of H_2, the *total* H_2 uptake at 110 bar and 77 K was calculated to be 135 mg/g (Figure 3C). The uptake of **NU-111** is within range of the DOE's revised long-term *systems* target for onboard H_2 storage, 5.5 wt % (58 mg/ g), albeit at cryogenic rather than ambient temperature. The simulated H_2 isotherm of **NU-111** was in only qualitative
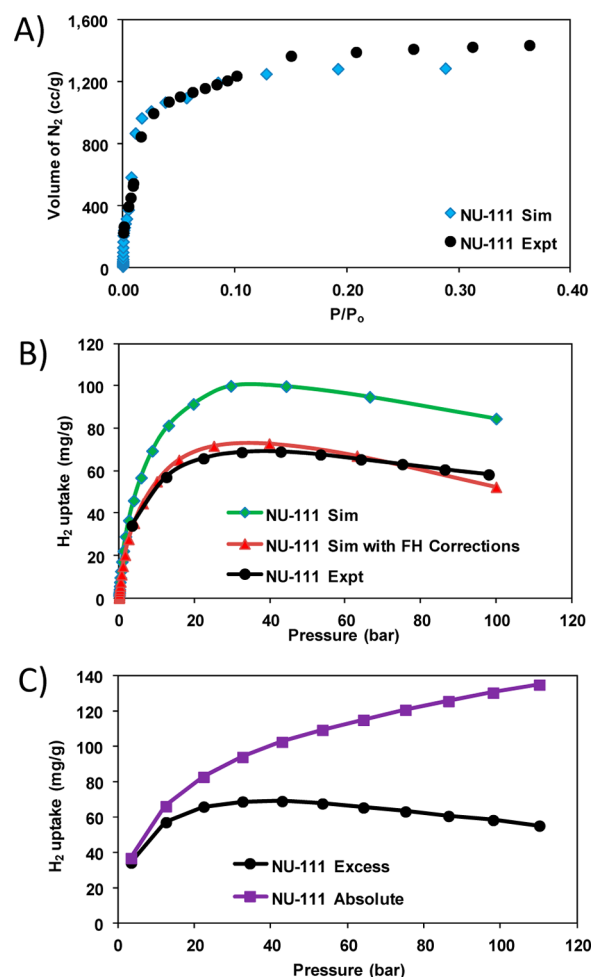
agreement with the experimental H_2 measurements using the classical force field model[34] (Figure 3B). Incorporating the Feynman–Hibbs (FH) corrections for quantum diffraction effects resulted in excellent agreement with the experimental isotherm.[35]

The stability of **NU-111** was examined by running multiple cycles of high-pressure hydrogen adsorption at room temperature (see the SI), and it showed no loss of capacity. In addition, the N_2 isotherms for **NU-111** were measured before sending the sample to NREL and upon receiving the sample back from NREL (see the SI). The N_2 isotherm showed no loss of porosity as a result of the shipping and measurements.

In conclusion, we have synthesized and characterized **NU-111**, a stable and promising material for hydrogen storage at cryogenic temperatures. **NU-111** was constructed from a linker whose arms each contain two triple-bond spacers in place of the one or two phenyl spacers in previously used linkers. Our results suggest that replacing the phenyl spacers with triple-bond spacers may be a better strategy than using longer linkers to obtain higher-surface-area MOFs. The experimental and simulated data for **NU-111** are in excellent agreement, which leads us to believe that a high-throughput computational screening approach, as recently described by Wilmer et al.[36] for the related problem of high-pressure methane storage, may be sufficiently accurate to identify excellent candidate MOFs for

high-pressure hydrogen storage. This may save experimentalists enormous amounts of time and effort as well as enable the efficient discovery and assessment of more promising MOFs such as **NU-111**.

■ ASSOCIATED CONTENT

ⓢ Supporting Information

General procedures, materials, and instrumentation; synthesis and characterization (^1H and ^{13}C NMR) of **LH$_6$(3)**; synthesis and X-ray crystallographic data (CIF) for **NU-111**; and sorption isotherms, BET analysis, and theoretical pore size distribution for **NU-111**. This material is available free of charge via the Internet at http://pubs.acs.org.

■ AUTHOR INFORMATION

Corresponding Author
o-farha@northwestern.edu; snurr@northwestern.edu; j-hupp@northwestern.edu

Author Contributions
‖O.K.F., C.E.W., and I.E. contributed equally.

Notes
The authors declare no competing financial interest.

■ ACKNOWLEDGMENTS

■ REFERENCES

(1) O'Keeffe, M.; Peskov, M. A.; Ramsden, S. J.; Yaghi, O. M. *Acc. Chem. Res.* **2008**, *41*, 1782.

(2) Férey, G. *Chem. Soc. Rev.* **2008**, *37*, 191.

(3) Horike, S.; Shimomura, S.; Kitagawa, S. *Nat. Chem.* **2009**, *1*, 695.

(4) Murray, L. J.; Dincă, M.; Long, J. R. *Chem. Soc. Rev.* **2009**, *38*, 1294.

(5) Hu, Y. H.; Zhang, L. *Adv. Mater.* **2010**, *22*, E117.

(6) Sculley, J.; Yuan, D.; Zhou, H.-C. *Energy Environ. Sci.* **2011**, *4*, 2721.

(7) Hu, Y.; Xiang, S.; Zhang, W.; Zhang, Z.; Wang, L.; Bai, J.; Chen, B. *Chem. Commun.* **2009**, 7551.

(8) Guo, Z.; Wu, H.; Srinivas, G.; Zhou, Y.; Xiang, S.; Chen, Z.; Yang, Y.; Zhou, W.; O'Keeffe, M.; Chen, B. *Angew. Chem., Int. Ed.* **2011**, *50*, 3178.

(9) Li, J.-R.; Kuppler, R. J.; Zhou, H.-C. *Chem. Soc. Rev.* **2009**, *38*, 1477.

(10) An, J.; Geib, S. J.; Rosi, N. L. *J. Am. Chem. Soc.* **2010**, *132*, 38.

(11) Bae, Y.-S.; Farha, O. K.; Hupp, J. T.; Snurr, R. Q. *J. Mater. Chem.* **2009**, *19*, 2131.

(12) Britt, D.; Furukawa, H.; Wang, B.; Glover, T. G.; Yaghi, O. M. *Proc. Natl. Acad. Sci. U.S.A.* **2009**, *106*, 20637.

(13) Lee, J.; Farha, O. K.; Roberts, J.; Scheidt, K. A.; Nguyen, S. T.; Hupp, J. T. *Chem. Soc. Rev.* **2009**, *38*, 1450.

(14) Ma, L.; Abney, C.; Lin, W. *Chem. Soc. Rev.* **2009**, *38*, 1248.

(15) Kreno, L. E.; Leong, K.; Farha, O. K.; Allendorf, M.; Van Duyne, R. P.; Hupp, J. T. *Chem. Rev.* **2012**, *112*, 1105.

(16) An, J.; Rosi, N. L. *J. Am. Chem. Soc.* **2010**, *132*, 5578.

(17) Horcajada, P.; Gref, R.; Baati, T.; Allan, P. K.; Maurin, G.; Couvreur, P.; Férey, G.; Morris, R. E.; Serre, C. *Chem. Rev.* **2012**, *112*, 1232.

(18) Lee, C. Y.; Farha, O. K.; Hong, B. J.; Sarjeant, A. A.; Nguyen, S. T.; Hupp, J. T. *J. Am. Chem. Soc.* **2011**, *133*, 15858.

(19) Kent, C. A.; Mehl, B. P.; Ma, L.; Papanikolas, J. M.; Meyer, T. J.; Lin, W. *J. Am. Chem. Soc.* **2010**, *132*, 12767.

(20) Getman, R. B.; Bae, Y.-S.; Wilmer, C. E.; Snurr, R. Q. *Chem. Rev.* **2012**, *112*, 703.

(21) Suh, M. P.; Park, H. J.; Prasad, T. K.; Lim, D.-W. *Chem. Rev.* **2012**, *112*, 782.

(22) http://www.caranddriver.com/news/mercedes-benz-f125-concept-auto-shows (accessed March 17, 2012).

(23) Nouar, F.; Eubank, J. F.; Bousquet, T.; Wojtas, L.; Zaworotko, M. J.; Eddaoudi, M. *J. Am. Chem. Soc.* **2008**, *130*, 1833.

(24) Farha, O. K.; Yazaydın, A. Ö.; Eryazici, I.; Malliakas, C. D.; Hauser, B. G.; Kanatzidis, M. G.; Nguyen, S. T.; Snurr, R. Q.; Hupp, J. T. *Nat. Chem.* **2010**, *2*, 944.

(25) Yuan, D.; Zhao, D.; Sun, D.; Zhou, H.-C. *Angew. Chem., Int. Ed.* **2010**, *49*, 5357.

(26) Yan, Y.; Lin, X.; Yang, S.; Blake, A. J.; Dailly, A.; Champness, N. R.; Hubberstey, P.; Schröder, M. *Chem. Commun.* **2009**, 1025.

(27) Yuan, D.; Zhao, D.; Zhou, H.-C. *Inorg. Chem.* **2011**, *50*, 10528.

(28) Yan, Y.; Yang, S.; Blake, A. J.; Lewis, W.; Poirier, E.; Barnett, S. A.; Champness, N. R.; Schroder, M. *Chem. Commun.* **2011**, *47*, 9995.

(29) Furukawa, H.; Ko, N.; Go, Y. B.; Aratani, N.; Choi, S. B.; Choi, E.; Yazaydın, A. Ö.; Snurr, R. Q.; O'Keeffe, M.; Kim, J.; Yaghi, O. M. *Science* **2010**, *329*, 424.

(30) Nelson, A. P.; Farha, O. K.; Mulfort, K. L.; Hupp, J. T. *J. Am. Chem. Soc.* **2008**, *131*, 458.

(31) Farha, O. K.; Hupp, J. T. *Acc. Chem. Res.* **2010**, *43*, 1166.

(32) Klein, N.; Senkovska, I.; Baburin, I. A.; Grünker, R.; Stoeck, U.; Schlichtenmayer, M.; Streppel, B.; Mueller, U.; Leoni, S.; Hirscher, M.; Kaskel, S. *Chem.—Eur. J.* **2011**, *17*, 13007.

(33) Han, D.; Jiang, F.-L.; Wu, M.-Y.; Chen, L.; Chen, Q.-H.; Hong, M.-C. *Chem. Commun.* **2011**, *47*, 9861.

(34) Levesque, D.; Gicquel, A.; Darkrim, F. L.; Kayiran, S. B. *J. Phys.: Condens. Matter.* **2002**, *14*, 9285.

(35) Liu, J.; Culp, J. T.; Natesakhawat, S.; Bockrath, B. C.; Zande, B.; Sankar, S. G.; Garberoglio, G.; Johnson, J. K. *J. Phys. Chem. C* **2007**, *111*, 9305.

(36) Wilmer, C. E.; Leaf, M.; Lee, C. Y.; Farha, O. K.; Hauser, B. G.; Hupp, J. T.; Snurr, R. Q. *Nat. Chem.* **2012**, *4*, 83.